

The Quark-Gluon Vertex in Landau gauge QCD

Markus Hopfer*

Karl-Franzens-University Graz

E-mail: markus.hopfer@uni-graz.at

Andreas Windisch

Karl-Franzens-University Graz

E-mail: andreas.windisch@uni-graz.at

Reinhard Alkofer

Karl-Franzens-University Graz

E-mail: reinhard.alkofer@uni-graz.at

The coupled system of the quark-gluon vertex and quark propagator Dyson-Schwinger equations (DSEs) is investigated within Landau gauge QCD. The aim is to get a deeper insight into the mechanisms of quark confinement and dynamical chiral symmetry breaking and into a possible relation between these two phenomena. To this end an earlier study is extended by improving systematically on the truncations imposed on the quark-gluon vertex DSE. A clear infrared enhancement for all tensor structures of the quark-gluon vertex is obtained.

*Xth Quark Confinement and the Hadron Spectrum,
October 8-12, 2012
TUM Campus Garching, Munich, Germany*

*Speaker.

1. Motivation

The mechanisms behind the most prominent features of QCD, namely confinement and dynamical chiral symmetry breaking (D χ SB), are still not completely understood. Moreover, a possible relation between these two phenomena is by no means obvious. Nevertheless, lattice simulations [1, 2] performed at finite temperature show that the corresponding phase transitions lie remarkably close together, which is a surprising result since the confinement phase transition, indicated by a breaking of center symmetry, is mainly driven by gluodynamics as pointed out in [3], whereas strong quark interactions seem to be responsible for the chiral phase transition. Moreover, a certain quark-gluon interaction strength is needed in order to generate mass dynamically in the infrared region. The aim is to shed more light on these effects by studying the quark-gluon vertex since this object is the link between the Yang-Mills and the matter sector of the theory. As both phenomena are related to the low-energy region of the theory a non-perturbative framework is necessary in addition to perturbative techniques. Dyson-Schwinger equations (DSEs) are an appropriate tool to explore the theory over a wide scope of momenta ranging from the deep infrared up to the perturbative regime, see *e.g.*, ref. [4, 5] and references therein. They build up to an infinite tower of coupled integral equations such that carefully chosen truncations have to be applied in order to evaluate the equations. Therefore, at some point a cooperation with other non-perturbative methods such as lattice simulations is necessary in order to render the Dyson-Schwinger framework reliable and robust and to acquire results which might be too difficult to obtain from a lattice calculation.

In these proceedings we extend previous studies of the quark-gluon vertex [6, 7] by systematically improving on the employed truncations. The starting point is the coupled system of the quark propagator and quark-gluon vertex DSE at vanishing temperatures in the Landau gauge using as input for the gluon propagator either fits [6, 8, 9] or results from a self-consistent treatment of the corresponding system of DSEs [10].¹ The three-gluon vertex model used in [6, 7] has been modified in order to take recent lattice results [13] into account.

Although the ghost propagator does not enter directly the DSEs for the quark propagator and the quark-gluon vertex one has to note that the infrared suppression of the gluon propagator is a direct consequence of the the infrared enhancement of the ghost propagator (see *e.g.*, ref. [14]). The resulting positivity violation for transverse gluons identifies the role of the transverse gluons in a non-perturbative BRST quartet mechanism [15] and thus a partial aspect of gluon confinement: In Landau gauge QCD transverse gluons are confined and therefore not confining. Consequently, due to the infrared suppression of the gluon propagator the quark-gluon vertex has to acquire a certain strength in the infrared to provide D χ SB or maybe even the infrared divergence indicating quark confinement. Within the truncation of ref. [6] (and at vanishing temperatures and densities) D χ SB and quark confinement occur either together in a self-consistent way or are both absent.

An improved truncation of the quark-gluon vertex DSE might give deeper insights into the

¹These fits correspond to a so-called scaling solution, one of two solution types of Landau gauge Green functions when classified by their infrared properties, see *e.g.*, ref. [11] and references therein. However, we want to stress the evidence that the differences of these types of solutions in the far infrared are irrelevant for phenomenological results. Furthermore, using numerical input obtained from a self-consistent solution of the corresponding Yang-Mills system leaves additional freedom in taking novel findings from other investigations, see *e.g.*, ref. [12], into account.

possible relation between quark confinement and $D\chi SB$. In addition, isolating important tensor structures of the quark-gluon vertex will provide a guidance when modeling this object in phenomenological applications. In particular, corresponding investigations at non-vanishing temperatures and/or quark chemical potentials involving the quark-gluon vertex can benefit from a better understanding of the vertex structure, see *e.g.*, ref. [16].

2. The coupled system of equations

The coupled system of equations for the quark propagator and the quark-gluon vertex is depicted in Fig. 1 and serves as a starting point for this investigation. The equation for the quark-

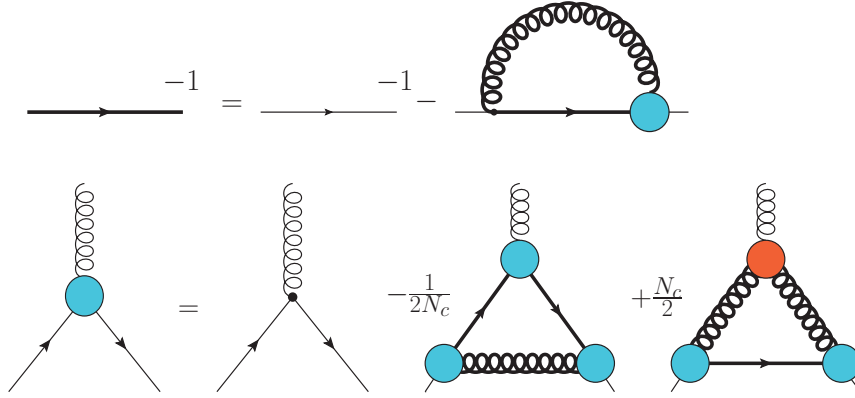


Figure 1: The quark propagator and the quark-gluon vertex DSE. All internal propagators are dressed. The vertex equation has been derived from a 3PI effective action [17]. The color prefactors of the Abelian- and the non-Abelian diagram are shown explicitly.

gluon vertex has been derived from a 3PI effective action and corresponds to the DSE truncated at three-point level [6, 17]. Note that all vertices are dressed due to the nPI-based approach. The last two diagrams on the right-hand side of the vertex equation are referred to as the *Abelian* and the *non-Abelian* diagram. The color traces yield a prefactor of $N_c/2$ for the non-Abelian diagram, whereas the Abelian diagram is suppressed by a factor of $-1/2N_c$. This natural N_c^2 difference between the two diagrams has been found to be even more severe due to the dynamics of the system [6].² Indeed, the simplest possible self-consistent treatment of the system reveals a suppression of the Abelian diagram by two orders of magnitude compared to the non-Abelian diagram. In this scenario the quark-gluon vertex DSE has been treated within a *leading order skeleton expansion*, i.e. all dressed vertices on the right-hand side of the vertex equation are substituted by their bare counterparts. We note however that in this setting the resulting feed-back on the propagator, i.e. the effective quark-gluon interaction strength, is not strong enough to trigger $D\chi SB$. This result on the one hand confirms previous DSE studies [18, 6] and on the other hand makes the necessity

²Furthermore, one can argue that the two dressed quark propagators in the Abelian diagram act as an additional damping factor not only for very heavy quarks but also in the chiral limit via $D\chi SB$. Of course, only a detailed investigation of the Abelian diagram in upcoming studies will reveal whether this naive argument also holds in a self-consistent treatment of the system.

obvious to treat the quark-gluon vertex DSE in a self-consistent manner including at least the most important tensor structures relevant for $D\chi SB$ in order to generate mass dynamically.

Thus, the road map towards a self-consistent solution of the system depicted in Fig. 1 contains the following points. In a previous first step only parts of the non-Abelian diagram have been taken into account [7], whereas in these proceedings now the full non-Abelian diagram has been included into the calculations. A detailed investigation of the Abelian diagram within a self-consistent treatment will be performed in an upcoming study.

2.1 Towards a self-consistent solution

Since previous investigations of the system indicate a possible dominance of the non-Abelian diagram, the following simplified system depicted in Figs. 2 and 3 has been considered as a first step towards the full solution of the more complicated system given in Fig. 1. Using an even

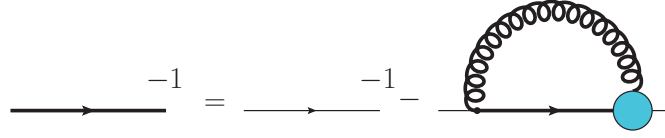


Figure 2: The quark propagator DSE coupled to a full quark-gluon vertex DSE denoted by the blue blob. The gluon propagator has been taken as input from external DSE calculations [6, 8, 10].

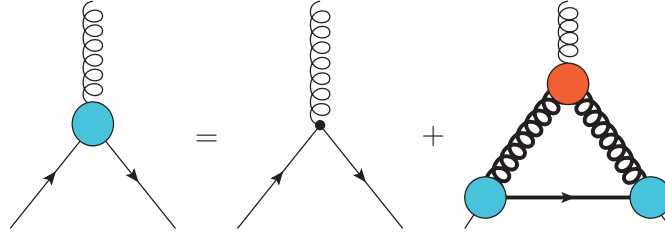


Figure 3: The truncated quark-gluon vertex DSE including the full non-Abelian diagram. For the three-gluon vertex model a modified version compared to the one used in [6, 7] has been employed.

simpler approximation, a similar system has been treated previously [7]. But in addition to [7] now the full non-Abelian diagram has been included. In Fig. 3, the complete tensor structure is coupled back to the full vertex, where this object also enters the quark propagator equation in Fig. 2. We employ twelve tensor structures to span the vertex, where it turned out to be numerically advantageous to use a simple basis given by

$$\Gamma^\mu(p, q) \propto \left\{ \begin{array}{c} \mathbb{1} \\ \not{p} \\ \not{q} \\ \frac{1}{2}[\not{p}, \not{q}] \end{array} \right\} \otimes \left\{ \begin{array}{c} \gamma^\mu \\ p^\mu \\ q^\mu \end{array} \right\}$$

instead of the widely-used Ball-Chiu basis [19].³ Here, p and q are the in- and outgoing quark momenta. As input from the Yang-Mills sector a gluon propagator has been employed which is

³A more efficient way to arrange the basis elements can be found in [20]. This choice of basis setting will be employed in upcoming studies. We thank Richard Williams and Gernot Eichmann for discussions and useful hints.

quenched and of scaling type [6, 8, 10].⁴ Here we note that instead of using fits [6] for the gluon propagator, it is convenient to include this object also from a direct calculation [10] since this step leaves the possibility to take more recent findings for the Yang-Mills system into account, see *e.g.*, [12, 13, 21, 22] and references therein.

For the three-gluon vertex in Fig. 3 a similar approach as in [12] has been employed. It is given by the tree-level tensor structure of this object combined with the following bose-symmetric ansatz

$$\Gamma^{3g}(x) = - \left(\frac{x}{d_1 + x} \right)^{-3\kappa} \left(\frac{d_1}{d_1 + x} \right)^4 + d_2 \log \left[\frac{x}{2} + 1 \right]^{17/44} \quad (2.1)$$

where $x = p_1^2 + p_2^2 + p_3^2$ is the sum over the squared momenta entering the vertex and $\kappa \approx 0.595$. This ansatz inherits the strong infrared enhancement known from Yang-Mills theory (see however the footnote in Sec.1) as well as ensures the correct anomalous dimension of the vertex in the UV region. The novel improvement compared to [6, 7] is the zero crossing for small momenta such that Γ^{3g} becomes negative for small momenta. This behavior is strongly indicated by recent lattice calculations performed in two, three and four space-time dimensions, see [12] for a detailed discussion. In two space-time dimensions, the results show a zero crossing such that the three-gluon vertex becomes negative [23] and are furthermore in agreement with the expected scaling behavior [24], whereas in three and four dimensions no scaling solution has been found on the lattice so far. Thus, the three-gluon vertex might approach a negative but finite value in the infrared regime in these cases as pointed out in [12]. Unfortunately in four space-time dimensions the statistics is not yet high enough to draw definite conclusions about the deep infrared region and therefore future lattice calculations are needed to clarify this issue. Nevertheless, the vertex is suppressed towards small momenta and shows qualitative agreement with the three-dimensional case where this suppression is even more pronounced and a clear sign flip has been observed [13].⁵ Therefore we included this property also in our model for the three-gluon vertex. In addition, we show in Sec. 3 that no stable solution could have been obtained without performing this step. Additionally, the model inherits two residual parameters d_1 and d_2 which have to be fixed to physical observables, *e.g.* the chiral condensate.

2.2 Obtaining the vertex dressing functions

Here, we follow the procedure as proposed in [7]. As a first step, a disentanglement of the dressing functions is necessary in order to get them in an explicit form. Since the employed basis is neither orthonormal nor orthogonal a linear system of equations for the vertex dressing functions has to be solved which can be calculated in advance yielding explicit expressions for the dressing functions as linear combinations of the twelve right-hand side projections. The algebraic

⁴It can be shown that unquenching effects play a minor role at vanishing temperatures [9]. Nevertheless, studying the back-reaction of quarks on the Yang-Mills sector by replacing the usual Ball-Chiu- or Curtis-Pennington vertex constructions with a full self-consistent quark-gluon vertex would be an interesting task. In particular when going to finite chemical potential and temperature in future calculations this step will become mandatory. Furthermore, we want to stress again that a gluon propagator of decoupling type could be employed here as well since the deep infrared behavior of the Yang-Mills system should not affect the phenomenological results.

⁵Furthermore, due to the qualitative similarity of the propagators in three and four space-time dimensions there is evidence that the zero crossing might also occur in four space-time dimensions as pointed out in [12].

manipulations have been performed with the program FORM [25]. During each iteration step these projections are calculated numerically, and subsequently, are plugged into the solution of the pre-calculated linear system in order to obtain the vertex dressing functions.

2.3 Renormalization and numerical treatment

The renormalization procedure is performed analogous to [7], except that the renormalization constant Z_{1F} in front of the non-Abelian diagram is now absent due to the 3PI structure of the vertex equation. The mass renormalization constant Z_m , the quark wave function renormalization constant Z_2 as well as the quark-gluon vertex renormalization constant Z_{1F} in front of the bare vertex have been fixed within a momentum subtraction (MOM) scheme. In particular, the renormalization constants are fixed by the conditions $A(\mu^2) = \lambda_1(\mu^2, \mu^2, 2\mu^2) = 1$, where μ^2 denotes some large renormalization scale. Note that only λ_1 , corresponding to the tree-level part γ^ν , has to be treated in the renormalization process since all other tensor structures lead to UV finite integrals due to the power-like suppression of the corresponding contributions at large momenta. Furthermore, the condition $B(\mu^2) = m_R$ fixes the constant Z_m , where m_R is the mass at the renormalization scale.

The evaluation of the coupled system depicted in Fig. 2 and Fig. 3 is numerically expensive. Thus, the actual calculations are performed on Graphics Processing Units (GPUs) using CUDATM and openMPI. In fact, the parallelization of the problem is straightforward since a decomposition into independent smaller fractions is possible. Each vertex dressing function $\lambda_{i=1\dots 12}(p^2, q^2, p \cdot q)$ depends on three variables. Therefore, we employ a coarse grained parallelization using openMPI corresponding to the external momentum p^2 in the quark propagator. On each GPU a fine grained parallelization using CUDATM has been employed which performs the subsequent integrals for all twelve dressing functions and the particular value of p^2 . After this step the synchronization and the evaluation of the linear system for the dressing functions takes place. The advantage of this procedure is the minimized communication between the individual processes and the scaling to an, in principle, arbitrary number of GPUs.⁶

3. Results

The system described in Sec. 2.1 has been solved self-consistently, taking all twelve tensor structures for the quark-gluon vertex into account. Due to stability issues it was in our previous study [7] not possible to take the complete non-Abelian diagram as well as the full infrared strength of the three-gluon vertex $(p^2)^{-3\kappa}$ into account as can be seen in Fig. 4(a) which shows the behavior of the mass function $M(p^2)$ as obtained from the quark propagator dressing functions in the chiral limit. Here, the corresponding infrared exponent of the three-gluon vertex has been varied from 0 to -2κ resulting in moderate changes of the dynamically generated mass (dashed lines). The solid line shows the dynamically generated mass as obtained from the full treatment of the system described in Sec. 2.1. Fig. 4(b) shows the dimensionless vertex dressing functions λ_1 , λ_2 and λ_3 which correspond to the tensor structures γ^ν , p^ν and $-q^\nu$ evaluated at the symmetric point $p^2 = q^2$ and $p \cdot q = 0$. We note that we observe the significant infrared enhancement also for the other

⁶In fact, the number of GPUs is limited only by the size of the external momentum grid, which ranges from 32 to 64 Gauss-Legendre nodes in our calculations.

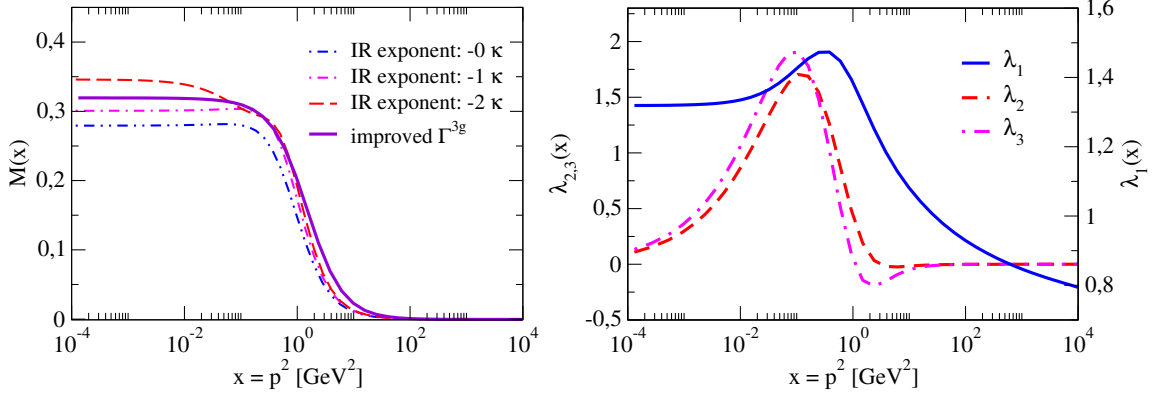


Figure 4: Left: The solid line shows the mass function $M(p^2) = B(p^2)/A(p^2)$ as obtained from the coupled system presented in Sec. 2.1. The dashed lines correspond to a previous treatment of the system [7] including only a partially dressed non-Abelian diagram. Here, the infrared exponent of the employed three-gluon vertex model [6, 7] has been varied, where no stable solutions could have been obtained for values larger than -2κ . Right: The dimensionless vertex dressing functions λ_1 , λ_2 and λ_3 corresponding to the tensor structures γ^ν , p^ν and $-q^\nu$ of the quark-gluon vertex evaluated at $p^2 = q^2$ and $p \cdot q = 0$.

vertex tensor structures, independent whether they are invariant under chiral transformations or are non-invariant and thus (in the chiral limit) generated dynamically via $D\chi\text{SB}$. Furthermore, the decoupling type of solution seen in the calculations might be attributed to a different initialization strategy of the vertex dressing functions as compared to the one in ref. [6].

4. Conclusions and outlook

The coupled system of quark propagator and quark-gluon vertex has been investigated in Landau gauge using a Dyson-Schwinger approach. Results for the quark propagator coupled the quark-gluon vertex DSE including the full non-Abelian diagram have been presented. An enhancement in the infrared regime has been observed in most of the quark-gluon vertex dressing functions leading to an effective quark-gluon interaction strength strong enough to generate mass dynamically. The isolation of relevant tensor structures seems feasible and will be investigated in an upcoming study of the system, where additionally the influence of the Abelian diagram within a dynamical setup will be investigated, thus aiming towards a complete solution of the system as depicted in Fig. 1. Isolating important tensor structures and thus a reduction of complexity is also mandatory in studies involving the quark-gluon vertex, especially those at non-vanishing temperatures and/or quark chemical potentials.

Acknowledgments

We thank Gernot Eichmann, Christian Fischer, Markus Q. Huber, Manfred Liebmann, Felipe Llanes-Estrada, Mario Mitter and Richard Williams for helpful discussions. MH and AW acknowledge support by the Doktoratskolleg "Hadrons in Vacuum, Nuclei and Stars" of the Austrian Science Fund, FWF DK W1203-N16. This study is also supported by the Research Core Area "Modeling and Simulation" of the University of Graz, Austria.

References

- [1] F. Karsch and E. Laermann, In *Hwa, R.C. (ed.) et al.: Quark gluon plasma* 1-59 [hep-lat/0305025].
- [2] Y. Aoki, Z. Fodor, S. D. Katz and K. K. Szabo, Phys. Lett. B **643** (2006) 46 [hep-lat/0609068].
- [3] J. Braun, L. M. Haas, F. Marhauser and J. M. Pawłowski, Phys. Rev. Lett. **106** (2011) 022002 [arXiv:0908.0008 [hep-ph]].
- [4] R. Alkofer and L. von Smekal, Phys. Rept. **353** (2001) 281 [arXiv:hep-ph/0007355].
- [5] P. Maris and C.D. Roberts, Int. J.Mod. Phys. E**12** (2003) 297 [arXiv:nucl-th/0301049].
- [6] R. Alkofer, C. S. Fischer, F. J. Llanes-Estrada and K. Schwenzer, Annals Phys. **324** (2009) 106 [arXiv:0804.3042 [hep-ph]].
- [7] A. Windisch, M. Hopper and R. Alkofer, arXiv:1210.8428 [hep-ph].
- [8] C. S. Fischer and R. Alkofer, Phys. Lett. B **536** (2002) 177 [hep-ph/0202202].
- [9] C. S. Fischer and R. Alkofer, Phys. Rev. D **67** (2003) 094020 [hep-ph/0301094].
- [10] M. Hopper, R. Alkofer and G. Haase, Comput. Phys. Commun., in press (available online) [arXiv:1206.1779 [hep-ph]].
- [11] C. S. Fischer, A. Maas and J. M. Pawłowski, Annals Phys. **324** (2009) 2408 [arXiv:0810.1987 [hep-ph]].
- [12] M. Q. Huber and L. von Smekal, arXiv:1211.6092 [hep-th]; PoS CONFINEMENTX (2013) 062 [arXiv:1301.3080 [hep-th]].
- [13] A. Cucchieri, A. Maas and T. Mendes, Phys. Rev. D **77** (2008) 094510 [arXiv:0803.1798 [hep-lat]].
- [14] P. Watson and R. Alkofer, Phys. Rev. Lett. **86** (2001) 5239 [hep-ph/0102332].
- [15] N. Alkofer and R. Alkofer, Phys. Lett. B **702** (2011) 158 [arXiv:1102.2753 [hep-th]]; PoS QCD-TNT-II (2011) 002 [arXiv:1112.4483 [hep-th]].
- [16] M. Hopper, M. Mitter, B.-J. Schaefer and R. Alkofer, arXiv:1211.0166 [hep-ph].
- [17] J. Berges, Phys. Rev. D **70** (2004) 105010 [hep-ph/0401172].
- [18] F. J. Llanes-Estrada, C. S. Fischer and R. Alkofer, Nucl. Phys. Proc. Suppl. **152** (2006) 43 [hep-ph/0407332].
- [19] J. S. Ball and T. -W. Chiu, Phys. Rev. D **22** (1980) 2542.
- [20] G. Eichmann and C. S. Fischer, arXiv:1212.1761 [hep-ph].
- [21] R. Alkofer, C. S. Fischer and F. J. Llanes-Estrada, Phys. Lett. B **611** (2005) 279 [Erratum-ibid. **670** (2009) 460] [hep-th/0412330].
- [22] R. Alkofer, M. Q. Huber and K. Schwenzer, Eur. Phys. J. C **62** (2009) 761 [arXiv:0812.4045 [hep-ph]].
- [23] A. Maas, Phys. Rev. D **75** (2007) 116004 [arXiv:0704.0722 [hep-lat]].
- [24] M. Q. Huber, A. Maas and L. von Smekal, JHEP **1211** (2012) 035 [arXiv:1207.0222 [hep-th]].
- [25] J. A. M. Vermaseren, math-ph/0010025.